



AutoATES v2.0: Automated avalanche terrain exposure scale mapping

Håvard B. Toft^{1,2*}, John Sykes^{3,4}, Andrew Schauer⁴, Jordy Hendrikx^{5,6,2} and Audun Hetland²

¹ Norwegian Water Resources and Energy Directorate, Oslo, Norway

5 ² Center for Avalanche Research and Education, UiT the Arctic University of Norway, Tromsø, Norway

³ SFU Avalanche Research Program, Department of Geography, Simon Fraser University, Canada

⁴ Chugach National Forest Avalanche Center, Girdwood, AK, USA

⁵ Antarctica New Zealand, Christchurch, New Zealand

⁶ Department of Geosciences, UiT the Arctic University of Norway, Tromsø, Norway

10

**Corresponding author address:*

Håvard B. Toft, Norwegian Water Resources and Energy Directorate, Oslo, Norway; tel:

+47 454 82 195; email: htla@nve.no

15

Keywords: ATES, GIS, snow, avalanche,

Throughout the paper, we will use the terms: model and algorithm interchangeably, but they convey the same meaning.

20

Abstract

This paper documents substantial improvements to the original automated avalanche terrain exposure mapping (AutoATES v1.0) algorithm. The most significant drawbacks of AutoATES v1.0 have been addressed by including forest density data, improving the avalanche runout estimations in low-angle runout zones, accounting for overhead exposure and open-source software. The algorithm also supports the new ATES v2.0 terrain class 'extreme' terrain. We used two benchmark maps from Bow Summit and Connaught Creek to validate the improvements from AutoATES v1.0 to v2.0. For Bow Summit, the F1 score (a measure of how well the algorithm performs) improved from 64.01% to 77.30%. For Connaught Creek, the F1 score improved from 39.81% to 71.38%. The main challenge limiting large-scale mapping is the determination of optimal input parameters for different regions and climates. In areas where AutoATES v2.0 is applied, it can be a valuable tool for avalanche risk assessment and decision. Ultimately, our goal is for AutoATES v2.0 to enable efficient, large-scale, and potentially global ATES mapping in a standardized manner rather than based solely on expert judgement.

25

30

1. Introduction

35

Approximately 140 fatal accidents result from snow avalanches in Europe and Northern America annually (Techel et al., 2016, 2018; Birkeland et al., 2017). In recent decades, most of these fatalities have been related to the recreational use of avalanche terrain (Engeset et al., 2018). In 90% of cases, the victim or someone in their group triggered the avalanche (Schweizer and Lütschg, 2001). Many countries have established an avalanche forecasting service to increase awareness of and help mitigate the risk of avalanches and focus on increased public education (Engeset et al., 2018). Despite the availability of public regional avalanche forecasting in many countries, assessing the avalanche risk is a complex task for backcountry recreationists due to the spatial and temporal variability of snow. This results in a wicked learning environment, where feedback is not always reliable (Fisher et al., 2022). The avalanche risk is managed by performing detailed assessments of, i.e., weather, snowpack, and signs of instabilities at a regional scale. An efficient method to mitigate the avalanche hazard is using appropriate terrain for the avalanche conditions (Thumlert and Haegeli, 2017).

40

45

50

Assessing avalanche terrain may be intuitive for avalanche professionals (Landrø et al., 2020), however, this may not be the case for recreational users of avalanche terrain. The avalanche terrain exposure scale (ATES) is a terrain classification system developed by Parks Canada to communicate the complexities and risks of traveling in avalanche-prone terrain (Statham et al., 2006). ATES is a commonly used classification scheme



55 worldwide and quantifies the avalanche terrain into an easy-to-understand rating: simple (class 1),
challenging (class 2), and complex (class 3) terrain. A more detailed technical description of these classes is
presented in Statham et al. (2006) and also reproduced in Larsen et al., (2020). Recently, the ATES
classification scheme has been updated to include two additional ratings; non-avalanche (class 0, optional)
and extreme (class 4) terrain to complement the current ATES classes from 1-3 (Statham and Campbell,
2023).

60 Avalanche hazard mapping has been common practice for decades to calculate the potential consequence
of different avalanche scenarios related to infrastructure (Schläpky et al., 2013). The maps are often
calculated for a specific return period (i.e., the probability of a given magnitude avalanche every 100 years)
and determines the likelihood of an avalanche (sometimes with specific impact pressures) within a defined
area. The return periods vary by application, and by country (DIBK, 2017; BFF and SLF, 1984). In recent years,
65 it has become more common to undertake an assessment of avalanche terrain zoning, where the aim is to
divide the avalanche terrain into different zones or classes (e.g., ATES) depending on a specific skill level (CAA,
2016) or for recreational purposes (Campbell and Gould, 2013; Schmudlach and Köhler, 2016; Thumlert and
Haegeli, 2017; Harvey et al., 2018; Larsen et al., 2020; Schumacher et al., 2022). In addition to mapping to
inform users, ATES mapping has also been used as an important component to assess and measure terrain
use preferences of backcountry users using GPS at a range of spatial scales (e.g., Hendrikx et al., 2022;
70 Johnson & Hendrikx, 2021; Sykes et al., 2020). Statham et al. (2006) noted that the ultimate goal would be
to apply the ATES classification spatially to produce ATES maps across entire regions. From 2009 through
2012, Avalanche Canada mapped several thousand square kilometers of avalanche terrain (Campbell and
Gould, 2013). This mapping was undertaken using a combination of manual mapping and GIS-assisted
mapping workflows, which relied heavily on expert judgement. As part of this work, Campbell and Gould
75 (2013) identified the need for a more quantifiable model and suggested a new zonal ATES model for GIS-
assisted classification. Therefore, the majority of large-scale mapping of ATES have been limited by the
manual labor needed to generate maps. ATES is, therefore, typically only available in high-use areas due to
the number of resources needed to generate ATES maps.

80 The first attempt at a fully automated ATES classification was made by Larsen et al. (2020) using a
combination of the zonal and technical model of ATES (Campbell and Gould, 2013; Statham et al., 2006). The
authors developed an automated ATES (AutoATES v1.0) algorithm that produces spatial ATES maps for all of
Norway, using only a digital elevation model (DEM) as input. The main limitations of this work were that the
algorithm did not account for forest data, or overhead exposure, and the performance of the simple
85 avalanche runout simulation was insufficient in flat runouts. The algorithm was also heavily dependent on
proprietary software (Larsen et al., 2020), thereby increasing the monetary and computing costs to operate
the model, and also limiting open sources access.

90 In avalanche terrain zoning, the main goal is to divide the terrain into different zones or classes representing
different areas of hazard, using a defined classification scheme. Avalanche terrain, especially when complex
is the result of interactions of multiple release areas, tracks, and deposition areas. Within these three areas,
other factors, i.e., terrain traps or forest density, could make terrain management more complex due to a
more severe outcome. The two most important components in making a good avalanche terrain zoning
algorithm are the delineation of the start zone area, as defined by the potential release area (PRA) model,
95 and the avalanche runout distance and width, accounting for the track and deposition area. An increase in
accuracy in either of these components directly benefits avalanche terrain zoning models. Additional factors
like forest density have also been found to be significant (Delparte, 2008; Schumacher et al., 2022).

100 The use of an appropriate PRA model to delineate the start zones of avalanche paths, is critical when creating
a good avalanche terrain zoning model (Sykes et al., 2022). The PRA establishes the baseline for where
avalanches may release and is used as an input for the avalanche runout simulations. Manual classification
of PRAs is time-consuming and often involves field observations, historic events review, and numerical



105 simulations (Bühler et al., 2018). A range of different PRA algorithms based on GIS or remote sensing have been developed (Bühler et al., 2018, 2013; Maggioni and Gruber, 2003; Barbolini et al., 2011; Pistocchi and Notarnicola, 2013; Chueca Cía et al., 2014; Andres and Chueca Cia, 2012; Ghinoi and Chung, 2005; Veitinger et al., 2016).

110 The two most commonly used PRA algorithms are those developed by Bühler et al. (2013) and Veitinger et al. (2016). A key difference between the two algorithms is that the one from Bühler et al. (2013) produces a binary polygon-based output, while the one from Veitinger et al. (2016) produces a continuous raster layer ranging from 0 to 1. Both algorithms are considered to have a good performance, even though the polygon-based algorithm was found to be slightly more accurate (Bühler et al. 2018). In prior automated ATES mapping work, Larsen et al., (2020) used the PRA algorithm of Veitinger et al. 2016 for the AutoATES v1.0 algorithm due to the continuous raster output. It is possible to include a binary forest parameter in the
115 Veitinger et al (2016) PRA model. However, the binary nature of the parameter results in coarse output, as the model removes all PRAs when the forest parameter takes the value 1. Sharp (2018) improved this PRA algorithm by incorporating forest density as a parameter in the fuzzy logic operator, making the forest interaction more dynamic.

120 There are several avalanche runout simulation models available which, given specific start zone inputs from the PRA model, outputs the potential track and deposition area. In principle, these runout models could be divided into two categories: (1) process-based, which attempt to calculate all the physical properties involved, or (2) empirical models which is driven by data-based observations. Which modelling approach to choose depends on the problem to be solved, data availability, the required accuracy and the spatial scale
125 (D'Amboise et al., 2022). Given access to highly detailed data and unlimited computational power, the process-based models outperform the data-based empirical models. However, given the limitations in computational power when processing large areas and the need for more accurate DEMs in many countries, the data-based model is more suitable for large-scale mapping applications.

130 Two of the most common process-based simulation tools for avalanche hazard assessment are the RAMMS (Christen et al., 2010) and Samos-AT (Sampl and Zwinger, 2004) models. Both models are made to simulate an accurate prediction of avalanche runout distances, flow velocities and impact pressures in a 3-dimensional space. These models are typically calibrated towards known avalanches with long return periods and defines potential avalanche terrain. These models are suitable for avalanche terrain zoning, where the aim is to divide
135 the potential avalanche terrain into different zones, across large spatial areas such as regional forecast areas or entire countries, these models are less suitable.

In contrast to the process-based models, data-based models are computationally inexpensive and can more easily be applied to large geographic areas. A common data-based method to delineate avalanche runout is
140 applying the classical runout angle concepts and path routing in three-dimensional terrain (D'Amboise et al. 2022).

In prior automated ATES mapping work, Larsen et al. (2020), used the multiple flow direction algorithm D-infinity (Tarboton, 1997). This algorithm is coupled with the travel angle (i.e., alpha angle). The D-infinity
145 algorithm identifies the cells downslope of the starting cell for each PRA cell. The algorithm spreads downslope until a defined alpha angle is reached from the starting cell (as per Heim, 1932; Lied & Bakkehoi, 1980; Toft et al., 2023). While used in hydrology applications, a substantial weakness of the D-infinity algorithm is that it cannot appropriately model avalanche movement, which may occasionally flow in flat and uphill terrain.
150

Recently, D'Amboise et al. (2022) presented a new customizable simulation package (Flow-Py) to estimate the runout distance and intensity of avalanches. The model utilizes persistence-based routing instead of terrain-based routing, enabling the simulation to respond appropriately to flat or uphill terrain. Where the



155 D-infinity algorithm only considers flow direction, the Flow-Py algorithm also considers flow process intensity.
They use the same stopping criteria to estimate the runout distance by defining the alpha angle from the
initial starting cell.

2. Model motivation

160 The main objective of the AutoATES v2.0 algorithm is to improve large-scale spatial ATES mapping, update
the mapping to reflect recent changes in ATES which include the two new terrain classes (0 and 4), and
improve the model workflow. Manual ATES classification using avalanche experts is time-consuming and
expensive (Sykes et al., 2020), limiting large-scale mapping. For AutoATES v2.0 to be a viable option for large-
scale ATES classification, the model performance should, on average, be as accurate as manual mapping or
better.

165

2.1 Model description

This paper aims to document the improvements made to the AutoATES v1.0 algorithm initially developed
by Larsen et al. (2020). In AutoATES v2.0, the influence of the forest density has been included by
integrating the parameter into the PRA model (as per Sharp, 2018), track and the deposition area. The
170 TauDEM runout model (Tarboton, 2005), which is known to perform poorly in flat deposition areas (Larsen
et al. 2020), has been replaced by the new Flow-Py model (D'Amboise et al. 2022). Another advantage of
the Flow-Py model is a separate output layer which enables the model to quantify the overhead exposure
from multiple avalanche paths, which is an important consideration in the updated ATES model. Finally, the
model now also includes the new ATES class for extreme terrain (Statham and Campbell, 2023) and steps to
175 improve delineation of terrain traps.

2.2 Implementation

To secure a broad adaptation of the new AutoATES model it is important that the model is open-source and
easy to use. The v1.0 algorithm was written using proprietary software. We have resolved this by rewriting
180 the entire v2.0 algorithm into the programming language Python using widely available and open-source
modules. The AutoATES v2.0 model is available on GitHub (Toft, Sykes, et al., 2023).

2.3 Input data

185 The minimum input data required to run the full AutoATES v2.0 is a DEM and forest density raster, both
using the GeoTIFF format. It is also possible to run the algorithm with only a DEM as input, but the output
would then only be valid for open, non-vegetated terrain. Both rasters must have a matching spatial
resolution, extent and be defined using a projected coordinate system. The algorithm has been tested with
spatial resolutions ranging from 5 to 30 m (cell sizes), but it should be possible to run other spatial
resolutions.

190

Our parametrization for forest density allows for various metrics of forest density inputs. The algorithm is
designed to work with stem density, percent canopy cover, basal area and no forest (only for mapping of
open terrain). The forest type must be defined using a string in the beginning of the Python script ('stems',
'pcc', 'bav' and 'no_forest'). Forest density influences snow accumulation and snowpack stability, with
195 denser forests generally reducing the risk of avalanches.

2.3.1 Percent canopy cover

Canopy cover has a direct relationship with radiation balance and can impact formation of persistent weak
layers as well as give an estimate of the degree of snowfall intercepted by trees prior to falling onto the
200 snowpack. Percent canopy cover is a widely used metric that quantifies the extent of forest density by
measuring the proportion of the ground area obscured by tree canopies when viewed from above. Percent
canopy cover can be estimated using various methods, including aerial photography, satellite imagery,
remote sensing techniques, and ground-based measurements. The resultant parameter used in our model
has a value ranging from 0 to 100.



205

2.3.2 Stem density

Stem density is a metric used to quantify the number of tree stems (trunks) per unit area, typically expressed as stems per hectare or stems per square meter, which provides insight into forest structure and composition. Stem density can influence the snowpack stability and avalanche initiation, as a higher stem density generally results in more trees obstructing and anchoring the snow, thereby reducing the likelihood of avalanche occurrence. Stem density can be measured through various techniques, including field surveys, aerial imagery analysis, or remote sensing data. The resultant parameter used in our model can have a value ranging from 0 to infinity, and is stated in stem density per hectare.

210

215

2.3.3 Basal area

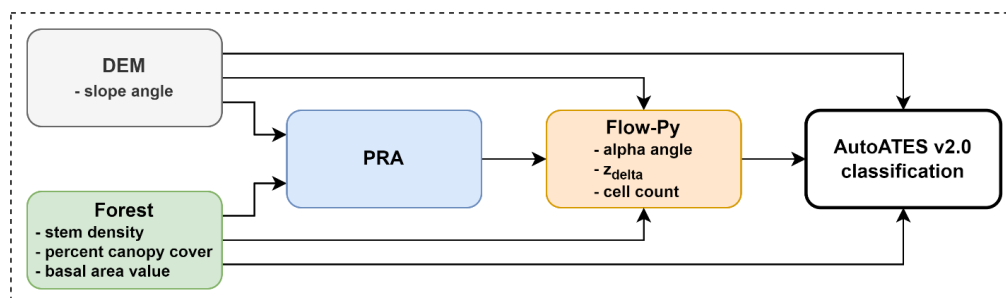
The basal area represents the total cross-sectional area of all living trees in the dominant, co-dominant, and high intermediate crown positions and is measured in m²/hectare (Sandvoss et al., 2005). The advantage over crown cover and stem density is that it incorporates the size of trees in addition to the number of trees and is a more direct measurement of the density of the forest vegetation. The resultant parameter used in our model can have a value ranging from 0 to infinity, and is stated in m² per hectare.

220

2.4 Model components

The AutoATES v2.0 algorithm is split into two main components: (1) pre-processing and (2) the AutoATES classifier. In the pre-processing step, the DEM and forest density rasters are used as input for the start zone PRA algorithm. When the PRA calculations are complete, the PRA and DEM is used to calculate the avalanche runout using the Flow-Py component. When all the key components are calculated, they are used as input for the AutoATES classifier which assigns the final ATES classes for each raster cell (Figure 1).

225



230

Figure 1: The main components of the AutoATES v2.0 algorithm. First, a pre-processing step is completed to calculate all the necessary raster layers using PRA and Flow-Py. Finally, the AutoATES classifier is used to assign the final ATES classifications.

2.4.1 PRA

The AutoATES v1.0 algorithm (Larsen et al., 2020) incorporated the PRA model developed by Veitinger et al. (2016) to calculate the potential release areas. This PRA model (v1.0) uses slope angle, roughness and windshelter as input parameters. Sharp (2018) modified this algorithm to also include forest density. The algorithms utilize Cauchy membership values to assign the importance of each parameter (Jang et al. 1997). A Cauchy membership values must be defined for each input variable (Eq. 1).

240

$$\mu(x) = \frac{1}{1 + \left(\frac{x-c}{a}\right)^{2b}} \quad (1)$$

where $\mu(x)$ is the Cauchy membership value, x is an input variable, and a , b , and c are parameters which control the weight of each input variable. We use the membership values suggested by Veitinger et al. (2016)



245 for slope angle and windshelter, while using the value suggested by Sharp (2018) for stem density (Figure 2).
 In our modified version of the PRA model (v2.0), we have chosen to remove the roughness parameter due to
 the scale issues with 5-30 m cell sizes. The removal of roughness makes it less ideal for higher resolution
 DEMs (< 5 m cell sizes). We also defined some new membership functions based on input from Parks Canada
 avalanche experts and through testing of the AutoATES model on our two study areas. These values could be
 fine-tuned for different inputs to improve the performance of the PRA model.

250

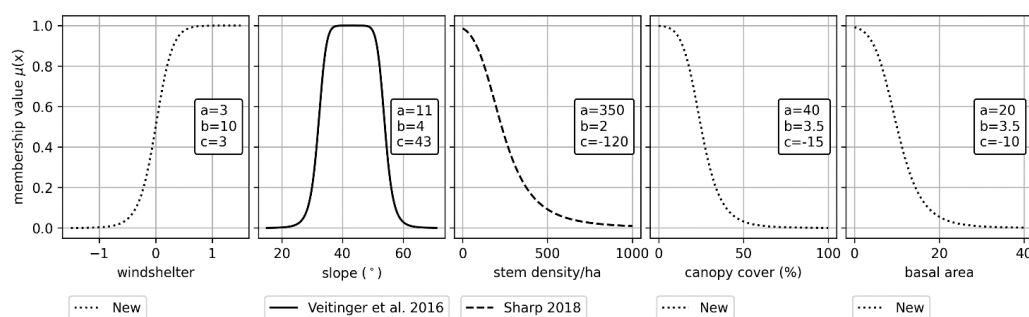


Figure 2: The different Cauchy functions used by Veitinger et al. (2016) and Sharp (2018) for slope angle and stem density. We have suggested new membership values for windshelter, canopy cover (%) and basal area. We recommend that these values are fine-tuned for specific datasets and applications, read a more in-depth discussion of this in section 4.3.

255

The Cauchy membership values from slope angle, windshelter and forest density is used as inputs for the fuzzy operator. We use the same “fuzzy AND” operator used by both Veitinger et al. (2016) and Sharp (2018), originally defined by Werners (1988). The PRA value is therefore defined as follows in Eq. 2:

260

$$\mu_{\text{PRA}}(x) = \gamma \cdot \min(\mu_s(x), \mu_w(x), \mu_f(x)) + \frac{(1-\gamma) + (\mu_s(x), \mu_w(x), \mu_f(x))}{3}, \quad (2)$$

$$x \in X, \gamma \in [0, 1]$$

265

With three fuzzy sets slope angle $\mu_s(x)$, windshelter $\mu_w(x)$, forest density $\mu_f(x)$ and with γ defined in Eq. 3 as:

$$\gamma = 1 - \min(\mu_s(x), \mu_w(x), \mu_f(x)) \quad (3)$$

270

The PRA output is a continuous layer ranging between 0 (not likely) to 1 (very likely). Most data-based runout models need release areas in a binary format where 0 is no potential release areas, while the potential release areas are encoded as 1. To convert the PRA layer to a binary format, we select a cut off threshold ($\text{PRA}_{\text{threshold}}$) where all pixels above this value is considered a potential release area for the runout modelling. We found the $\text{PRA}_{\text{threshold}}$ from Larsen et al. (2020) to be too conservative and have therefore increased the value to 0.15. The $\text{PRA}_{\text{threshold}}$ could be adjusted depending on whether frequent or more extreme avalanche scenarios are of interest.

275

280

We have also adjusted how the windshelter index is calculated. Using a 2m DEM, Veitinger et al. (2016) resampled the DEM by a factor of 5 (from 2m to 10m) and applied a 11x11 sliding window. This is according to the recommendations of Plattner et al. (2006) which found the optimal radius to be 60 meters, followed by a secondary optimal radius of 250 meters. To achieve the same results, we removed the down sampling factor of 5 and used the 10m DEM directly to calculate the windshelter index. If other DEM resolutions are to be used, the windshelter index should be adjusted accordingly to use either 60 m (recommended) or 250



m as the radius around each cell. This could be done by either resampling the spatial resolution or changing the size of the sliding window.

285

2.4.2 Avalanche simulation

The Flow-Py model developed by D’Amboise et al. (2022) is used for the avalanche simulation of the potential track and deposition area. It is similar to the TauDEM algorithm utilized in AutoATES v1.0 which uses the alpha angle to limit the flow (Larsen et al., 2020; Tarboton, 1997). Flow-Py also includes a flow process intensity parameter which makes it able to handle mass movement in flat and uphill terrain, significantly improving the output compared to the previous model. Another advantage with the FlowPy model is the additional output layers which represents the overhead exposure. We utilize the cell count and Z_{delta} layer by scaling the two layers and taking their average value which represents the overhead exposure layer. In the AutoATES v2.0 algorithm it is possible to select cell count, Z_{delta} or both to represent the overhead exposure. The layer enables us to quantify the exposure from different release areas at every raster cell. We use the forest detrainment module of Flow-Py which makes it possible to use forest density as an input layer to limit spreading and runout distance. An in-depth description of the Flow-Py simulation package can found in D’Amboise et al. (2022).

290

295

300

2.4.3 AutoATES classifier

When the pre-processing of PRA and Flow-Py is completed, the AutoATES classifier uses a set of map algebra equations to define each ATEs class. The following raster layers from the pre-processing step are used as input in the AutoATES classifier:

305

- Slope angle (calculated from the DEM)
- Forest density (provided by the user, as per section 2.3.1-2.3.3)
- PRA (calculated from the DEM)
- Runout distance as a function of alpha angle (calculated from PRA and Flow-Py)
- Overhead exposure (cell count, Z_{delta} or both) (calculated from PRA and Flow-Py)

310

The first step of the AutoATES classifier is controlled by adjustable thresholds for slope angle, runout distance, overhead exposure and island filter size (Table 1). Using these parameters, the AutoATES model outputs a preliminary, and conservative, layer with the categorical classes (1) simple, (2) challenging, (3) complex and (4) extreme terrain by keeping the maximum value between the 3 input rasters.

315

Table 1: The recommended input parameters for AutoATES according to Sykes et al. (2023). The encoding describes the name of each parameter in the AutoATES algorithm.

Input parameter	Class	Range	Encoding
Slope angle threshold (SAT)	Simple (1)	< 18°	SAT12=18°
	Challenging (2)	18 – 28°	SAT23=28°
	Complex (3)	28 – 39°	SAT34=39°
	Extreme (4)	> 39°	
Alpha angle threshold (AAT)	Simple (1)	< 24°	AAT12=24°
	Challenging (2)	24° – 33°	AAT23=33°
	Complex (3)	> 33°	
Overhead exposure (OE)	Simple (1)	< 50	OE12=50
	Challenging (2)	50 – 350	OE23=350
	Complex (3)	> 350	
Island filter size (ISL _{size})			30,000 m ²

320

The second step of the AutoATES classifier is to reduce the exposure in certain ATEs classes depending on forest density. The forest density is applied in a secondary step to increase the importance of the forest



density criteria. The forest density layers are divided into four different categories with different thresholds for each forest density input (Table 2).

325 Table 2: The recommended input parameters for AutoATES according to Sykes et al. (2023). The encoding describes the name of each parameter in the AutoATES algorithm. Only one of the forest inputs can be used at the time, the encoding is therefore identical for all three forest density types.

Input parameter	Class	Range	Encoding
Forest density (Percent canopy cover)	Open	0 – 20%	TREE1=20
	Sparse	20 – 55%	TREE2=55
	Moderate	55 – 75%	TREE3=75
	Dense	75 – 100%	
Forest density (stem density/ha)	Open	0 – 100	TREE1=100
	Sparse	100 – 250	TREE2=250
	Moderate	250 – 500	TREE3=500
	Dense	> 500	
Forest density (basal area)	Open	0 – 10	TREE1=10
	Sparse	10 – 20	TREE2=20
	Moderate	20 – 25	TREE3=25
	Dense	> 25	

330 Once the forest density parameter has been coded into the four classes of forest density (i.e., open, sparse, moderate and dense), as a function of the forest density input parameter used, we mapped these categorical descriptors on to ATEs classes (Table 3).

Table 3: Forest criteria applied to the second step of the AutoATES.

Forest criteria		Initial ATEs rating			
		Simple (1)	Challenging (2)	Complex (3)	Extreme (4)
Open	PRA & Runout	Simple (1)	Challenging (2)	Complex (3)	Extreme (4)
Sparse	PRA & Runout	Simple (1)	Simple (1)	Challenging (2)	Complex (3)
Moderate	PRA	Simple (1)	Simple (1)	Challenging (2)	Complex (3)
	Runout	Simple (1)	Simple (1)	Simple (1)	Complex (3)
Dense	PRA	Simple (1)	Simple (1)	Simple (1)	Challenging (2)
	Runout	Simple (1)	Simple (1)	Simple (1)	Complex (3)

335 Finally, the island filter size is applied removing clusters smaller than a specified area and incorporating it to the surrounding class. The filter size is not a new addition to the algorithm as it is a part of the v1.0 algorithm, but Sykes et al. (2023) found that a filter size of 30,000 m² (Table 1) was the optimal filter size for all the spatial resolutions tested. The additional step improves the accuracy of challenging (2) and complex (3) terrain, and in some cases in extreme (4) terrain.

340 2.5 AutoATES outputs

The outputs from AutoATES v2.0 have the same spatial resolution as the input. The following outputs are available:

- Continuous PRA
- 345 • Flow-Py raw outputs (D’Amboise et al. 2022).
- Preliminary ATEs classification of slope angle
- Preliminary ATEs classification of runout distance
- Preliminary ATEs classification of overhead exposure
- Forest density criteria



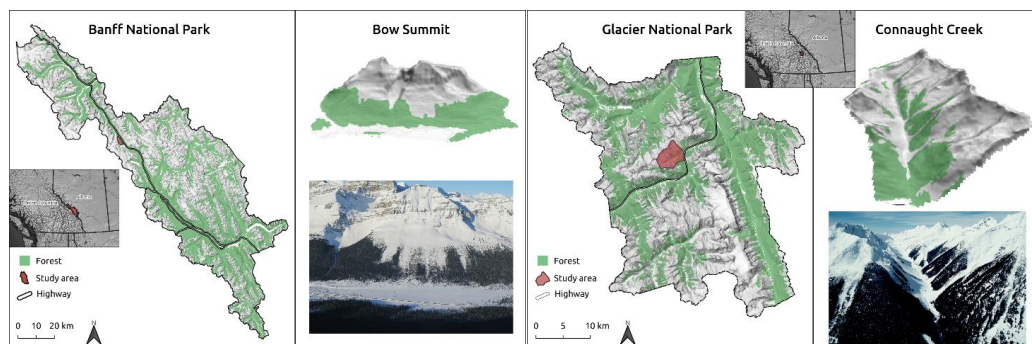
- 350
- AutoATES v2.0
 - AutoATES v2.0 with island size filter

2.6 Model assessment

355 Accuracy, precision, recall, and F1-score are essential metrics for evaluating the performance of a model. These metrics provide a more detailed assessment, accounting for class imbalance and varying prediction results. They have been widely used in various fields, including avalanche literature (e.g., Keskinen et al., 2022). For a more in-depth understanding of these metrics and their sources, see Liu et al. (2014), who provides a comprehensive review of evaluation metrics for classifiers.

360 3. Results and validation

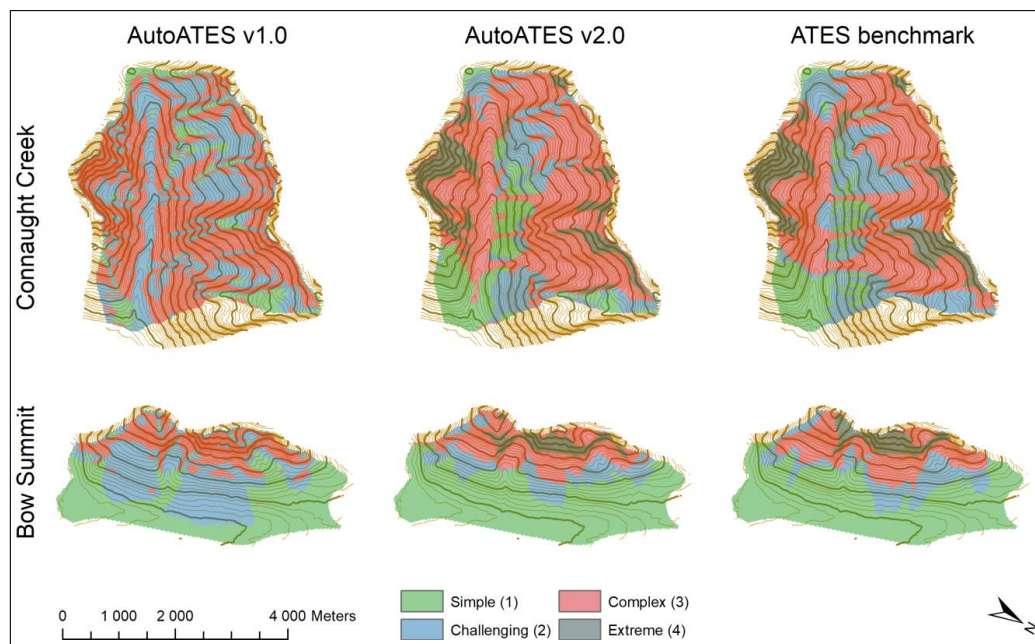
In order to evaluate the performance of AutoATES v2.0, we use two Canadian benchmark maps made explicitly for Connaught Creek, British Columbia and Bow Summit, Alberta Canada (Figure 3). These are the only locations that have manually mapped maps using the new 5 class ATES model (Statham and Campbell, 2023). The benchmark maps were made by combining individual maps from a panel of three experts, utilizing methodologies such as Geographic Information Systems (GIS), remote sensing imagery, local knowledge, and field-based investigations. Statham et al. (2023) provide an in-depth description of how the benchmark maps were developed.



370 Figure 3: Two areas where benchmark maps for the updated ATES are available is in Glacier and Banff National Park. An overview of the greater area with the study areas in 3D view and overview photo.

3.1. Model accuracy

375 There is no true validation dataset for AutoATES due to differences in scale between automated and manual methods, but we believe the new benchmark maps made by Sykes et al. (2023) provides the best spatial validation maps to date. In figure 4, we visualize the differences between AutoATES v1.0, v2.0 and the ATES benchmark maps for Connaught Creek and Bow Summit.



380 Figure 4: A visual comparison between AutoATES v1.0, v2.0 and the ATES benchmark maps for Connaught Creek and Bow Summit using the European ATES color scheme (Statham et al., 2023). AutoATES v1.0 does not use the extreme (4) class.

385 We use a confusion matrix for each study area to compare the ATES benchmark, which serves as the ground truth, against the results generated by the AutoATES v2.0 model (Table 4). The confusion matrices enable us to evaluate the performance of the AutoATES v2.0 model by calculating various metrics, such as accuracy, precision, recall, and F1-score. For Bow Summit, the algorithm performs really well for simple terrain with 91.97% accuracy, but the accuracy for challenging terrain is much lower at 65.34%. Complex and extreme terrain is closer to the average with an accuracy of 78.70% and 78.97% respectively (Table 4).
 390 The accuracy distribution between the four classes is slightly different for Connaught Creek. The v2.0 model performs the worst in simple terrain with an accuracy of 63.31%. Challenging terrain has an accuracy of 71.0%, complex has an accuracy of 78.0% and extreme terrain has an accuracy of 82.94% (Table 4).

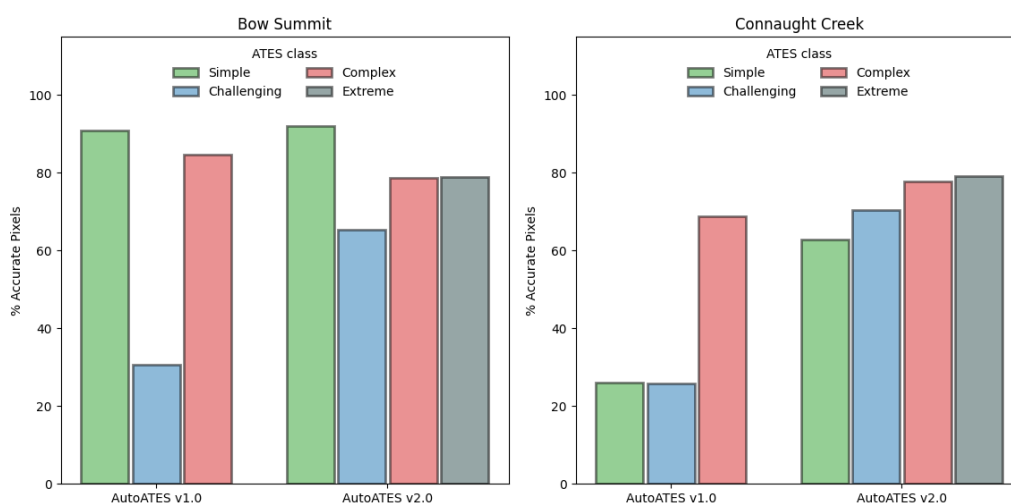
395 Table 4: A confusion matrix is used to compare the ATES benchmark maps with AutoATES v2.0. Bow Summit is presented above, while Connaught Creek is presented below. The accuracy of each terrain class is marked out with grey shading (area or percent of pixels correctly identified).

Bow Summit		AutoATES v2.0			
		Simple (1)	Challenging (2)	Complex (3)	Extreme (4)
ATES benchmark	Simple (1)	4,527,848 m ₂ (91.97%)	140,608 m ₂ (10.78%)	16,900 m ₂ (1.01%)	0 m ₂ (0.00%)
	Challenging (2)	391,404 m ₂ (7.95%)	852,436 m ₂ (65.34%)	179,816 m ₂ (10.75%)	0 m ₂ (0.00%)
	Complex (3)	4,056 m ₂ (0.08%)	310,960 m ₂ (23.83%)	1,316,172 m ₂ (78.70%)	110,188 m ₂ (21.03%)
	Extreme (4)	0 m ₂ (0.00%)	676 m ₂ (0.05%)	159,536 m ₂ (9.54%)	413,712 m ₂ (78.97%)
Connaught Creek					
ATES benchmark	Simple (1)	1,364,844 m ₂ (63.31%)	263,640 m ₂ (10.64%)	76,388 m ₂ (1.03%)	0 m ₂ (0.00%)
	Challenging (2)	683,436 m ₂ (31.30%)	1,757,600 m ₂ (70.96%)	884,208 m ₂ (11.92%)	676 m ₂ (0.05%)
	Complex (3)	102,752 m ₂ (4.77%)	449,540 m ₂ (18.15%)	5,787,236 m ₂ (78.00%)	237,276 m ₂ (17.01%)
	Extreme (4)	4732 m ₂ (0.22%)	6084 m ₂ (0.25%)	671,944 m ₂ (9.06%)	1,156,636 m ₂ (82.94%)



400 A visual presentation of the differences between the two models is shown in Figure 5 where a comparison shows how the models perform compared to the benchmark map for each ATES class, for Bow Summit and Connaught Creek. The bar sections show the absolute accuracy, which is the percentage of pixels that is identical between the benchmark and the automated map. In Bow Summit the v2.0 algorithm has improved challenging terrain a lot with a cost of a small reduction in accuracy of complex terrain. In Connaught Creek, the v2.0 algorithm has improved in all terrain classes, but the improvement is especially clear for simple and challenging terrain.

405



410 Figure 5: The figure shows how the new AutoATES v2.0 model performs compared to the benchmark maps for Bow Summit and Connaught Creek. The figure uses the European ATES color scheme (Statham et al., 2023). The bar sections show the absolute accuracy, which is the percentage of pixels that is identical between the benchmark and the automated map.

3.2 Ablation study

415 The performance of the AutoATES v2.0 model is a dramatic improvement as compared to AutoATES v1.0. The transition from v1.0 to v2.0 has been marked by numerous internal iterations, featuring improvements such as an optimized PRA algorithm accounting for forest data, incorporating the Flow-Py runout model, considering forest data in the final terrain class algorithm, and more. To fully understand the underlying factors behind the improvements of AutoATES v2.0, it is crucial to examine each of the components that have been modified, which will help clarify how each modification contributes to the overall performance of the algorithm.

420

To do this, we utilize the concept of an ablation study which is a common method used to evaluate the importance or contribution of individual components within a system, model, or algorithm. It is a type of sensitivity analysis that aims to understand the impact of removing or *ablating* specific components on the overall performance or output of the system. Ablation studies are commonly employed in machine learning, 425 computational neuroscience, and other scientific disciplines to analyze and understand the roles and relationships of different elements in a complex system (Meyes et al., 2019).

The general procedure for an ablation study involves the following steps:

- 430
1. Train or develop the full model or system with all its components and parameters intact, and measure its performance on a given task or dataset.



2. Systematically remove or disable one component or parameter at a time, keeping the rest of the model unchanged.
3. Measure the performance of the modified model without the removed component or parameter.
- 435 4. Compare the performance of the modified model to the performance of the original, complete model.
5. Repeat steps 2-4 for each component or parameter of interest.

For AutoATES v2.0, we have identified six components of the algorithm that have been developed since the v1.0. Using the concepts of an ablation study approach, we have calculated the precision, recall and F1-score by removing different components of the algorithm (Table 5). The reference model is the final AutoATES v2.0. The lower F1-score a model has compared to the reference, the more important is the component that has been removed. In Bow Summit, the most important component is the inclusion of forest data in the PRA algorithm (dev4). In Connaught Creek, the most important factor is the post-forest-classification (dev6). In general, all new components in AutoATES v2.0 improve the model by several percents, except the inclusion of AAT3 (dev2), which only improves by 0.08-0.14% for the two study areas.

Table 5: The results from the ablation study where different components are removed to measure the effect for Bow Summit.

	Version	Component removed	Pixel accuracy	Precision	Recall	F1-score	F1-score change
Bow Summit	v1.0*		67.40%	68.75%	66.07%	64.06%	-13.24 %
	dev1*	SAT34 threshold	87.63%	78.74%	76.05%	81.81%	4.51 %
	dev2	AAT3 threshold	84.20%	82.82%	80.97%	77.16%	-0.14 %
	dev3	Forest data from PRA v1.0	78.40%	78.6%	75.90%	70.21%	-7.09 %
	dev4	Forest data from PRA v2.0	76.80%	71.29%	70.61%	68.03%	-9.27 %
	dev5	Flow-Py (back to TauDEM)	79.10%	69.82%	68.99%	72.66%	-4.64 %
	dev6	Post-forest-classification	80.30%	73.38%	72.12%	75.49%	-1.81 %
v2.0	Reference		84.40%	75.74%	76.19%	77.30%	0.00 %
Connaught Creek	v1.0*		49.44%	40.21%	38.70%	38.70%	-32.68 %
	dev1*	SAT34 threshold	80.20%	72.43%	74.73%	72.79%	1.41 %
	dev2	AAT3 threshold	74.70%	73.65%	70.89%	71.30%	-0.08 %
	dev3	Forest data from PRA v1.0	71.80%	71.23%	64.12%	66.71%	-4.67 %
	dev4	Forest data from PRA v2.0	72.70%	73.33%	64.68%	67.73%	-3.65 %
	dev5	Flow-Py (back to TauDEM)	65.50%	66.78%	67.55%	65.87%	-5.51 %
	dev6	Post-forest-classification	59.90%	56.40%	48.20%	48.30%	-23.08 %
v2.0	Reference		74.90%	73.80%	70.94%	71.38%	0.00 %

450 * AutoATES v1.0 and dev1 uses the old ATES v1.0 framework with three terrain classes, which could lead to higher F1-scores. See section 4.1.1 for an in-depth discussion.

4. Discussion

455 One of the primary challenges when developing AutoATES v2.0 has been to create a robust process for validating the output. Initial attempts by Larsen et al., (2020) compared AutoATES v1.0 to available linear and spatial ATES ratings in Norway, but the validity of these layers was uncertain, given that multiple experts generated them, over a period of years, with limited review.

460 In contrast, the approach by Sykes et al., (2023), attempts to address these deficiencies, and create benchmark maps for two regions in Canada. Their approach, which used three human ATES mappers who independently mapped each study area, and then created benchmark maps based on their individual output through a detailed discussion of the terrain characteristics, is a more comprehensive methodology to address



this issue. For the purpose of our analysis, we consider these benchmark ATES maps as the standard to which we will measure any AutoATES models to.

465

When conducting our consensus matrices, we combine non-avalanche and simple terrain to make a 4-class validation dataset to be used against the AutoATES v2.0. We have chosen to not include a non-avalanche terrain class due to the challenges of defining non-avalanche terrain using automated methods.

470

While the benchmark maps provide the best available validation dataset there are still fundamental differences in how human mappers create ATES maps versus AutoATES. The scale of analysis for human mappers is generally focused on terrain features, classifying an entire ridgeline, bowl, or gully as a single unit of analysis. In contrast, AutoATES is a raster-based model which operates on a pixel-by-pixel analysis scale. The size of the pixels depends on the DEM data available for a given study area. Variability in DEM resolution and quality is one of the biggest challenges of applying AutoATES in data sparse regions, like Western Canada. The scale mismatch between human mapped ATES and AutoATES is a persistent difference and an issue that needs to be thoroughly considered with further validation efforts. The optimal scale of use for AutoATES is outside the scope of this current work, but detailed analysis by Sykes et al., (2023) has considered the impact of DEM resolution on AutoATES and notes that there is no real difference in performance using DEM datasets with a spatial resolution ranging from 5-26 m. We therefore recommend that the spatial resolution of the DEM and forest data is between 5 to 30 meters.

475

480

4.1 Model performance

We investigate the performance of the AutoATES v2.0 algorithm compared to the v1.0 model, both designed to identify potential release and runout areas. Although the underlying concept remains consistent between the two versions, numerous components have been altered or refined in the latest iteration.

485

4.1.1 Extreme terrain (dev1)

The first modification to the AutoATES v2.0 model was to include the extreme terrain class from ATES v2.0. We incorporated the new class by including another slope angle threshold (SAT). We measure the importance of this change by using the results from the ablations study (Table 5, dev1). The result is that the ablated model performs better with regards to F1-score (i.e., 4.51% improvement for Bow Summit, and 1.41% for Connaught Creek) than the reference model. This means that excluding the SAT34 threshold (i.e., complex / extreme threshold) increases the accuracy of the model. However, without it, the algorithm would be using the old ATES v1.0 classification excluding extreme terrain. This implies that excluding the SAT34 threshold enhances the model's numerical accuracy. Nonetheless, its absence would cause the algorithm to employ the outdated ATES v1.0 classification, which does not account for extreme terrain, and therefore diminishing its value for ATES v2.0.

490

495

When working with classification problems, decision boundaries are the borders or thresholds that separate different classes (Lee and Landgrebe, 1993). The complexity of the decision boundaries often depends on the number of classes. When there are fewer classes, the decision boundaries tend to be simpler, as there are fewer regions to separate in the feature space. With simpler decision boundaries, the model may have an easier time making accurate predictions, as there is less chance of overfitting or incorrectly assigning data points to the wrong class. This could lead to higher precision, recall, and ultimately higher F1 scores. We believe the fewer classes in the ATES v1.0 is the reason why it performs better than the ATES v2.0 reference model.

500

505

4.1.2 Terrain traps (dev2)

To improve the algorithms' ability to identify severe terrain traps such as depressions and gullies, another alpha angle threshold (AAT) was added to be included in complex terrain. The previous model only had AAT thresholds which defaulted terrain into simple and challenging terrain. The extra component was added in the early stages of the development of AutoATES v2.0. The ablation analysis show that this change has a very

510



1515 little effect on the overall performance of the model (Table 5, dev2). (i.e., 0.14% decrease for Bow Summit, and 0.08% for Connaught Creek)

4.1.3 Forest data in PRA (dev3 and dev4)

520 Forest density is considered to be one of the most important parameters for ATES classification. In the original PRA v1.0 from Veitinger et al. (2016) it was not possible to include forest density as one of the inputs. The modified PRA v2.0 used in the AutoATES v2.0 algorithm builds on the work from Sharp (2018).

525 The PRA was initially developed and optimized for a 2m DEM, while we utilize a 10m DEM as default. If roughness was calculated using a 10m DEM, it would measure the roughness at basin scale, instead of the roughness at the slope scale (Blöschl, 1999; Blöschl and Sivapalan, 1995). The roughness is also dependent of a snow depth value which is impossible to define without assessing the snowpack properties at a given time. We do not consider that there is value in running AutoATES v2.0 using high resolution DEMs (< 5 meter). Sykes et al., (2023) further illustrates the impact of DEM scale on ATES mapping. We have therefore chosen to remove the roughness parameter from our version of the PRA model.

530 When comparing the importance of PRA v1.0 (dev3) and PRA v2.0 (dev4) to the reference model, we see that the forest density into PRA is among one of the most important components (Table 5, dev3-4) (i.e., 7.09-9.27% decrease for Bow Summit, and 3.65-4.67% for Connaught Creek. Comparing the results between PRA v1.0 and PRA v2.0, we can measure the difference between the two models without forest input. We found that the PRA v1.0 performed better than v2.0 in Bow Summit, but the opposite is the case in Connaught
535 Creek. However, given that Larsen et al. (2020) did not adapt the PRA v1.0 algorithm according to the recommendations of Veitinger et al. (2016), we believe the changes are conceptually still important even though there are no substantial differences between the two in the ablation validation.

4.1.4 Flow-Py (dev5)

540 The previous iteration of AutoATES had some severe issues with the runout simulation of avalanches where avalanches were simulated using a flow model for water. The Flow-Py simulation works in a similar fashion where the flow is limited by an alpha angle threshold, but the flow model has been changed to give more realistic outputs in terms of snow avalanches. Some other advantages with the Flow-Py simulation suite are that there are additional outputs such as cell count and z_{delta} which makes it possible to account for the
545 exposure of multiple overlapping paths and avalanche paths with high kinetic energy. When we compare the Flow-Py outputs compared to the TauDEM, we see a substantial improvement when using the Flow-Py outputs (Table 5, dev5) (i.e., 4.64% decrease for Bow Summit, and 5.51% for Connaught Creek).

4.1.5 Post-forest-classification (dev6)

550 Even though the inclusion of forest density in the PRA algorithm improved the performance of AutoATES, we found the need to reclassify sections that obviously were densely forested and resulted in a higher ATES rating than needed. To improve this, we added a post-forest-classification criteria. This was really efficient for Connaught Creek, but less efficient for Bow Summit (Table 5, dev6) (i.e., 1.81% decrease for Bow, and 23.08% for Connaught Creek). The forest impact of dev6 is minimal at Bow Summit, but really important for
555 Connaught Creek. We don't know why this is, but one hypothesis is that there is more steep forested terrain in Connaught Creek, and the algorithm therefore relies more on the post-forest-classification. Connaught Creek also has more large runouts and overhead hazard that rely on the post-forest-classification.

560 In the future, we hope to be less reliant on the post-forest-classification criteria by optimizing the forest detrainment module in Flow-Py. This module of Flow-Py makes it possible to reduce the runout length in areas with dense forest.

4.1.6 Discrepancies



565 The discrepancy in accuracy scores between the two study areas is mainly attributed to the complex terrain
of Connaught Creek with many smaller topographical features and the limitations of the VRI forest data
resolution in capturing local forest characteristics (Sykes et al., 2023). This issue significantly affects the
assessment of overhead hazards and boundaries delineation between ATES classes, with challenging (2)
terrain showing the lowest accuracy and high rates of underprediction errors. Sykes et al. (2023) provides an
extended discussion of the differences between the two study sites.

570

4.3 Application

While it is possible to run the presented version of AutoATES v2.0 without making any changes, we
recommend a workflow where the optimal parameters are first identified. The suggested parameters in this
paper are valid for the two test areas in Western Canada, so when applying AutoATES v2.0, there will likely
575 need to be a reevaluate the parameters for the area being mapped. Blindly applying the parameters
presented in this document to other regions without site specific calibration risks inaccurate ATES mapping,
and potential catastrophic outcomes. Users should apply at their own risk. We therefore urge all future users
of our code to conduct, and document, their local validation before proceeding with the generation of ATES
maps, especially when the intended target is the general public.

580

Begin with a relevant test area which should include a variety of terrain and all terrain classes. We
recommend a workflow where the PRA model and Flow-Py is processed independent of the AutoATES
classifier. The output from PRA and Flow-Py is easier to validate by local experts compared to the AutoATES
output. It is more intuitive as avalanche experts have more tangible experience with identifying start and
585 runout zones. In our experience, we complete approximately 1-3 iterations of PRA and Flow-Py before
moving on to the AutoATES classifier. In general, we have experienced that the 'c' parameter in the Cauchy
function for slope angle combined with the max alpha angle for Flow-Py are the most effective for
customizing the output. We also recommend fine-tuning all parameters in the Cauchy function for PRA when
using new forest density data.

590

When these steps are done in advance, our experience is that the output of the AutoATES classifier tends to
be much more accurate. The final AutoATES could then be shared among local experts which provides further
feedback. Changes could then be made to the AutoATES classifier parameters and improved during an
iterative process. When the final input parameters are set, they could be used to generate larger areas. A
595 description of the input parameters used should be shared as meta-data with the resulting spatial maps.

4.4 Limitations

Despite the notable improvements of the AutoATES v2.0 model, there are still some limitations that should
be acknowledged.

600

- Flow-Py is computationally heavy, which may present challenges when processing large datasets or
applying the model in real-time applications. This could potentially limit the scalability and
accessibility of the model for certain use cases and users with limited computational resources.
- Determining the optimal input parameters for the AutoATES model is important to get the best
605 performance possible. The suitability of these parameters across different snow climates and terrain
types remains an open question. Further research and validation are needed to ensure that the
chosen parameters provide accurate and reliable results in various contexts. Users should not blindly
adopt the input parameters stated in this paper.
- The model does not account for changes in vegetation over time such as natural events like landslides
610 or forest fires. Therefore, it is important to update the ATES mapping periodically to account for
major changes in the landscape.



Addressing these limitations in future work could enhance the performance, applicability, and reliability of the AutoATES model, ensuring its effectiveness across a wide range climates and terrain characteristics.

615

5. Conclusion

In conclusion, the development of AutoATES v2.0 has focused on creating a more robust and accurate algorithm for mapping avalanche terrain into ATES ratings by incorporating new components to improve the algorithm. This has been achieved by integrating new components that enhance the algorithm's performance, including the addition of an extreme terrain class, improved PRA with support for multiple forest density types, Flow-Py, and a post-forest-classification criteria. Moreover, a significant portion of the code has been rewritten to increase efficiency and eliminate dependency on proprietary software.

620

However, limitations related to the determination of optimal input parameters for different regions and climates need to be considered for future model development. By addressing these limitations and continuing to refine the model through iterative testing and expert feedback, AutoATES v2.0 can serve as a valuable tool for avalanche risk assessment and decision-making in a wide range of snow climates and terrain types. Ultimately, our goal is for AutoATES v2.0 to enable efficient, large-scale, and potentially global ATES mapping in a standardized manner.

625

630

6. Code and data availability

To reproduce the results from this study, please find the AutoATES v2.0 algorithm and validation data from the ablation study in the [OSF repository](#). For future application of AutoATES v2.0, a [GitHub repository](#) will be maintained with future iterations of the algorithm available (Toft et al. 2023).

635

7. Author contribution

HT was the developer of the first version of automated ATES. The new versions improvements have been led by HT with significant contributions from JS and AS. The ablation study has been carried out by HT with inputs from JS. HT prepared the final manuscript with JH and AH as editors. All co-authors contributed to the final manuscript.

640

8. Competing interests

The authors declare that they have no conflict of interest.

645

9. References

- Andres, J. and Chueca Cia, J.: Mapping of avalanche start zones susceptibility: Arazas basin, Ordesa and Monte Perdido National Park (Spanish Pyrenees), *J Maps*, 8, 14–21, 2012.
- Barbolini, M., Pagliardi, M., Ferro, F., and Corradeghini, P.: Avalanche hazard mapping over large undocumented areas, *Natural Hazards*, 56, 451–464, <https://doi.org/10.1007/S11069-009-9434-8>, 2011.
- BFF and SLF: Richtlinien zur Berücksichtigung der Lawinengefahr bei raumwirksamen Tätigkeiten, Eidgenössische Drucksachen- und Materialzentrale, 42, 1984.
- Birkeland, K. W., Greene, E. M., and Logan, S.: In Response to Avalanche Fatalities in the United States by Jekich et al, *Wilderness Environ Med*, 28, 380–382, <https://doi.org/10.1016/j.wem.2017.06.009>, 2017.
- Blöschl, G.: Scaling issues in snow hydrology, *Hydrol Process*, 13, 2149–2175, [https://doi.org/10.1002/\(SICI\)1099-1085\(199910\)13:14/15<2149::AID-HYP847>3.0.CO;2-8](https://doi.org/10.1002/(SICI)1099-1085(199910)13:14/15<2149::AID-HYP847>3.0.CO;2-8), 1999.
- Blöschl, G. and Sivapalan, M.: Scale issues in hydrological modelling: A review, *Hydrol Process*, 9, 251–290, <https://doi.org/10.1002/hyp.3360090305>, 1995.
- Bühler, Y., Kumar, S., Veitinger, J., Christen, M., and Stoffel, A.: Automated identification of potential snow avalanche release areas based on digital elevation models, *Natural Hazards and Earth System Sciences*, 13, 1321–1335, <https://doi.org/10.5194/nhess-13-1321-2013>, 2013.
- Bühler, Y., von Rickenbach, D., Stoffel, A., Margreth, S., Stoffel, L., and Christen, M.: Automated snow avalanche release area delineation – validation of existing algorithms and proposition of a new object-

660



- based approach for large-scale hazard indication mapping, *Natural Hazards and Earth System Sciences*, 18, 3235–3251, <https://doi.org/10.5194/nhess-18-3235-2018>, 2018.
- 665 CAA: Technical Aspects of Snow Avalanche Risk Management – Resources and Guidelines for Avalanche Practitioners in Canada (C. Campbell, S. Conger, B. Gould, P. Haegeli, B. Jamieson, & G. Statham Eds.), Canadian Avalanche Association, 2016.
- Campbell, C. and Gould, B.: A proposed practical model for zoning with the Avalanche Terrain Exposure Scale, in: *International Snow Science Workshop Proceedings, Grenoble – Chamonix Mont-Blanc*, 385–391, 670 2013.
- Christen, M., Kowalski, J., and Bartelt, P.: RAMMS: Numerical simulation of dense snow avalanches in three-dimensional terrain, *Cold Reg Sci Technol*, 63, 1–14, <https://doi.org/10.1016/j.coldregions.2010.04.005>, 2010.
- 675 Chueca Cía, J., Andrés, A. J., and Montañés Magallón, A.: A proposal for avalanche susceptibility mapping in the Pyrenees using GIS: the Formigal-Peyreget area (Sheet 145-I; scale 1:25.000), *J Maps*, 10, 203–210, <https://doi.org/10.1080/17445647.2013.870501>, 2014.
- D’Amboise, C. J. L., Neuhauser, M., Teich, M., Huber, A., Kofler, A., Perzl, F., Fromm, R., Kleemayr, K., and Fischer, J.-T.: Flow-Py v1.0: a customizable, open-source simulation tool to estimate runoff and intensity of gravitational mass flows, *Geosci Model Dev*, 15, 2423–2439, <https://doi.org/10.5194/gmd-15-2423-2022>, 680 2022.
- Delparte, D. M.: Avalanche terrain modeling in Glacier National Park, Canada, PhD thesis, 1–195, <https://doi.org/10.1007/s13398-014-0173-7.2>, 2008.
- DIBK: Byggteknisk forskrift (TEK17), Kommunal- og distriktsdepartementet, 2017.
- Engeset, R. V., Pfuhl, G., Landrø, M., Mannberg, A., and Hetland, A.: Communicating public avalanche warnings – what works ?, *Natural Hazards and Earth System Science*, 18, 2537–2559, 685 <https://doi.org/https://doi.org/10.5194/nhess-18-2537-2018>, 2018.
- Fisher, K. C., Haegeli, P., and Mair, P.: Exploring the avalanche bulletin as an avenue for continuing education by including learning interventions, *Journal of Outdoor Recreation and Tourism*, 37, 100472, <https://doi.org/10.1016/J.JORT.2021.100472>, 2022.
- 690 Ghinoi, A. and Chung, C.-J.: STARTER: a statistical GIS-based model for the prediction of snow avalanche susceptibility using terrain features—application to Alta Val Badia, Italian Dolomites, *Geomorphology*, 66, 305–325, <https://doi.org/10.1016/j.geomorph.2004.09.018>, 2005.
- Harvey, S., Sch mudlach, G., Bühler, Y., Dürr, L., Stoffel, A., and Christen, M.: Avalanche Terrain Maps For Backcountry Skiing in Switzerland, in: *International Snow Science Workshop Proceedings, Innsbruck, Austria*, 1625–1631, 2018.
- 695 Heim, A.: *Bergsturz und Menschenleben*, Zürich, Fretz und Wasmuth, 1932.
- Hendrikx, J., Johnson, J., and Mannberg, A.: Tracking decision-making of backcountry users using GPS tracks and participant surveys, *Applied Geography*, 144, 102729, <https://doi.org/10.1016/J.APGEOG.2022.102729>, 2022.
- 700 Johnson, J. and Hendrikx, J.: Using Citizen Science to Document Terrain Use and Decision-Making of Backcountry Users, *Citiz Sci*, 6, <https://doi.org/10.5334/cstp.333>, 2021.
- Keskinen, Z., Hendrikx, J., Eckerstorfer, M., and Birkeland, K.: Satellite detection of snow avalanches using Sentinel-1 in a transitional snow climate, *Cold Reg Sci Technol*, 199, 103558, <https://doi.org/10.1016/j.coldregions.2022.103558>, 2022.
- 705 Landrø, M., Hetland, A., Engeset, R. V., and Pfuhl, G.: Avalanche decision-making frameworks: Factors and methods used by experts, *Cold Reg Sci Technol*, 170, 102897, <https://doi.org/10.1016/j.coldregions.2019.102897>, 2020.
- Larsen, H. T., Hendrikx, J., Slåtten, M. S., and Engeset, R. V.: Developing nationwide avalanche terrain maps for Norway, *Natural Hazards*, 103, <https://doi.org/10.1007/s11069-020-04104-7>, 2020.
- 710 Lee, C. and Landgrebe, D. A.: Decision boundary feature extraction for nonparametric classification, *IEEE Trans Syst Man Cybern*, 23, 433–444, <https://doi.org/10.1109/21.229456>, 1993.
- Lied, K. and Bakkehoi, S.: Empirical calculations of snow avalanche run-out distances based on topographic parameters, *Journal of Glaciology*, 26, 165–177, 1980.



- 715 Maggioni, M. and Gruber, U.: The influence of topographic parameters on avalanche release dimension and frequency, *Cold Reg Sci Technol*, 37, 407–419, [https://doi.org/10.1016/S0165-232X\(03\)00080-6](https://doi.org/10.1016/S0165-232X(03)00080-6), 2003.
- Meyes, R., Lu, M., de Puiseau, C. W., and Meisen, T.: Ablation studies in artificial neural networks, arXiv preprint, 2019.
- Pistocchi, A. and Notarnicola, C.: Data-driven mapping of avalanche release areas: a case study in South Tyrol, Italy, *Natural Hazards*, 65, 1313–1330, <https://doi.org/10.1007/s11069-012-0410-3>, 2013.
- 720 Plattner, C., Braun, L., and Brenning, A.: The spatial variability of snow accumulation at Vernagtferner, Austrian Alps, in winter 2003/2004, *Z. Gletscherk., Glazialgeol.*, 39, 43–57, 2006.
- Sampl, P. and Zwinger, T.: Avalanche simulation with SAMOS, *Ann Glaciol*, 38, 393–398, <https://doi.org/10.3189/172756404781814780>, 2004.
- Sandvoss, M., McClymont, B., and Farnden, C.: A user's guide to the vegetation resources inventory, Tolko Industries, Ltd.: Williams Lake, BC, Canada., 2005.
- 725 Schläppy, R., Jomelli, V., Grancher, D., Stoffel, M., Corona, C., Brunstein, D., Eckert, N., and Deschatres, M.: A New Tree-Ring-Based, Semi-Quantitative Approach for the Determination of Snow Avalanche Events: use of Classification Trees for Validation, *Arct Antarct Alp Res*, 45, 383–395, <https://doi.org/10.1657/1938-4246-45.3.383>, 2013.
- 730 Schmuldach, G. and Köhler, J.: Method for an automatized avalanche terrain classification, in: Proceedings, International Snow Science Workshop - Breckenridge, Colorado, 729–736, 2016.
- Schumacher, J., Toft, H., McLean, J. P., Hauglin, M., Astrup, R., and Breidenbach, J.: The utility of forest attribute maps for automated Avalanche Terrain Exposure Scale (ATES) modelling, *Scand J For Res*, 37, 264–275, <https://doi.org/10.1080/02827581.2022.2096921>, 2022.
- 735 Schweizer, J. and Lütschg, M.: Characteristics of human-triggered avalanches, *Cold Reg Sci Technol*, 33, 147–162, [https://doi.org/10.1016/S0165-232X\(01\)00037-4](https://doi.org/10.1016/S0165-232X(01)00037-4), 2001.
- Sharp, E.: Evaluating the exposure of heliskiing ski guides to avalanche terrain using a fuzzy logic avalanche susceptibility model, University of Leeds, Leeds, 2018.
- 740 Statham, G. and Campbell, C.: The Avalanche Terrain Exposure Scale v2.0, [Manuscript in preparations], 2023.
- Statham, G., McMahon, B., and Tomm, I.: The Avalanche Terrain Exposure Scale, International Snow Science Workshop Proceedings, Telluride, Colorado, 491–497, 2006.
- Sykes, J., Hendrikx, J., Johnson, J., and Birkeland, K. W.: Combining GPS tracking and survey data to better understand travel behavior of out-of-bounds skiers, *Applied Geography*, 122, <https://doi.org/10.1016/j.apgeog.2020.102261>, 2020.
- 745 Sykes, J., Haegeli, P., and Bühler, Y.: Automated snow avalanche release area delineation in data-sparse, remote, and forested regions, *Natural Hazards and Earth System Sciences*, 22, 3247–3270, <https://doi.org/10.5194/nhess-22-3247-2022>, 2022.
- 750 Sykes, J., Toft, H., Haegeli, P., and Statham, G.: Automated Avalanche Terrain Exposure Scale (ATES) mapping - Local validation and optimization in Western Canada, [Manuscript submitted for publication], 2023.
- Tarboton, D. G.: A new method for the determination of flow directions and upslope areas in grid digital elevation models, *Water Resour Res*, 33, 309–319, <https://doi.org/10.1029/96WR03137>, 1997.
- 755 Tarboton, D. G.: Terrain analysis using digital elevation models (TauDEM), Utah State University, Logan, 2005.
- Techel, F., Jarry, F., Kronthaler, G., Mitterer, S., Nairz, P., Pavšek, M., Valt, M., and Darms, G.: Avalanche fatalities in the European Alps: long-term trends and statistics, *Geogr Helv*, 71, <https://doi.org/10.5194/gh-71-147-2016>, 2016.
- 760 Techel, F., Mitterer, C., Ceaglio, E., Coléou, C., Morin, S., Rastelli, F., and Purves, R. S.: Spatial consistency and bias in avalanche forecasts -a case study in the European Alps, *Natural Hazards and Earth System Sciences*, 18, 2697–2716, <https://doi.org/10.5194/nhess-18-2697-2018>, 2018.
- Thumlert, S. and Haegeli, P.: Describing the severity of avalanche terrain numerically using the observed terrain practices of professional guides, *Natural Hazards*, 1–27, <https://doi.org/10.1007/s11069-017-3113-y>, 2017.



- 765 Toft, H. B., Sykes, J. M., and Schauer, A.: AutoATES v2.0, <https://github.com/AutoATES>, 2023.
Toft, H. B., Müller, K., Hendrikx, J., Jaedicke, C., and Bühler, Y.: Can big data and random forests improve avalanche runout estimation compared to simple linear regression?, *Cold Reg Sci Technol*, 211, 103844, <https://doi.org/10.1016/j.coldregions.2023.103844>, 2023.
- 770 Veitinger, J., Purves, R. S., and Sovilla, B.: Potential slab avalanche release area identification from estimated winter terrain: a multi-scale, fuzzy logic approach, *Natural Hazards and Earth System Sciences*, 16, 2211–2225, <https://doi.org/10.5194/nhess-16-2211-2016>, 2016.
Werners, B.: Aggregation models in mathematical programming, *Mathematical Models for Decision Support*, 48, 295–305, 1988.